Dirac vs. Weyl in topological insulators: Adler-Bell-Jackiw anomaly in transport phenomena

Heon-Jung Kim (Daegu Univ.), Ki-Seok Kim (POSTECH), J.-F. Wang (Huazhong Univ.), M. Sasaki (Yamagata Univ.), N. Satoh (Iwaki Meisei Univ.), A. Ohnishi, M. Kitaura, M. Yang, L. Li

arXiv:1307.6990

Claim: Observation of Weyl metal

Figure 1(a) Schematic band structure of $Bi_{1-x}Sb_x$ near the L point

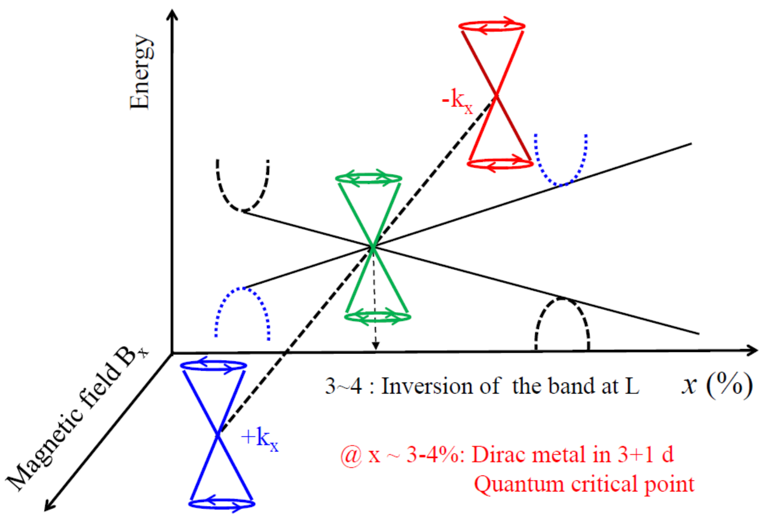

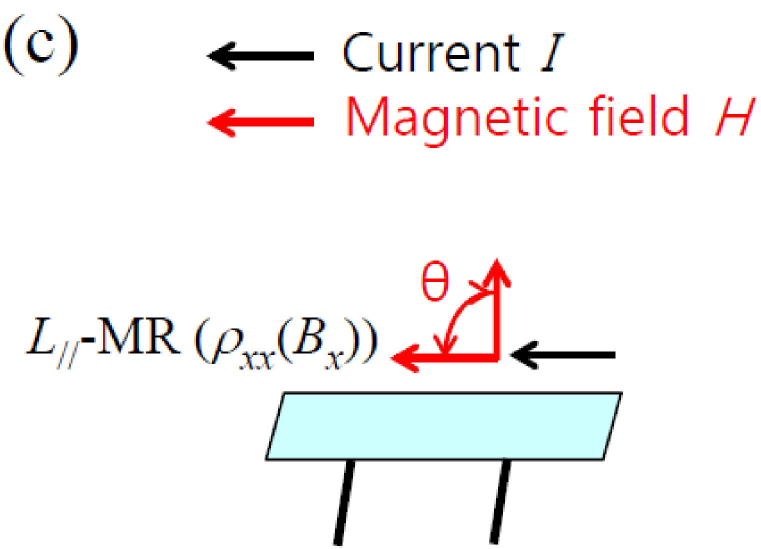

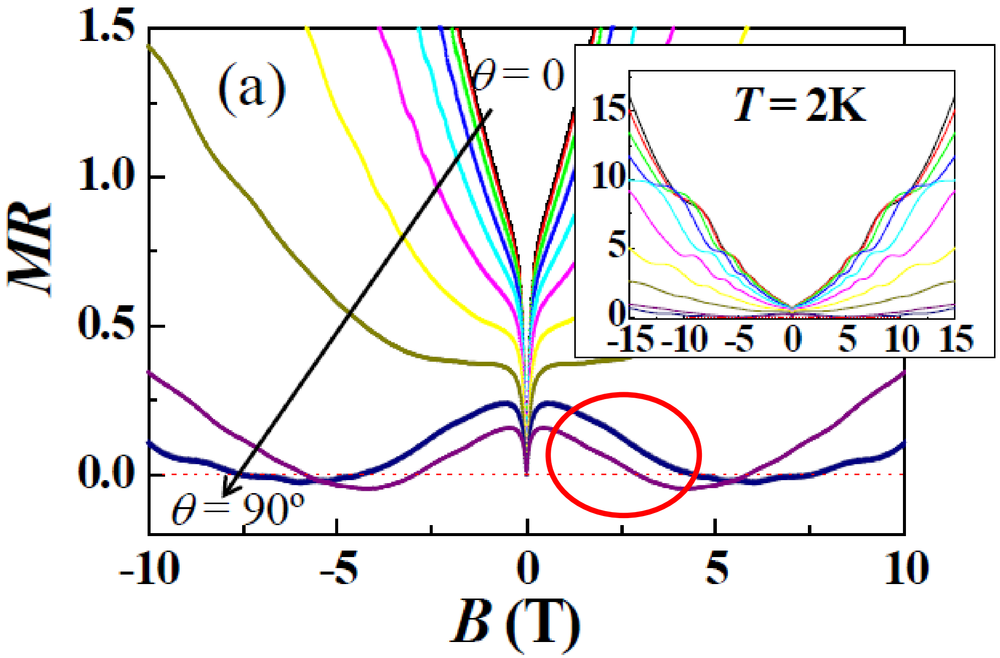

Adler-Bell-Jackiw anomaly

Two cornerstones in modern condensed matter physics

Symmetry ★ Topology

"Topological" Landau Fermi liquid theory ??
"Topological" Landau-Ginzburg framework
for phase transitions ??

Motivation: Toward interacting topological states of matter → Topological metal

Weyl Semimetal in a Topological Ins

Selected for a Viewpoint in *Physics*

PHYSICAL REVIEW B **83**, 205101 (2011)

Topological semimetal and Fermi-arc surface states in the electronic structure

Xiangang Wan,[1] Ari M. Turner,[2] Ashvin Vishwanath,[2,3] and Sergey Y. Savrasov[1,4]
[1]*National Laboratory of Solid State Microstructures and Department of Physics, Nanjing University, Nanjing 210093, China*
[2]*Department of Physics, University of California, Berkeley, California 94720, USA*
[3]*Materials Sciences Division, Lawrence Berkeley National Laboratory, Berkeley, California 94720, USA*
[4]*Department of Physics, University of California, Davis, One Shields Avenue, Davis, California 95616, USA*
(Received 23 February 2011; published 2 May 2011)

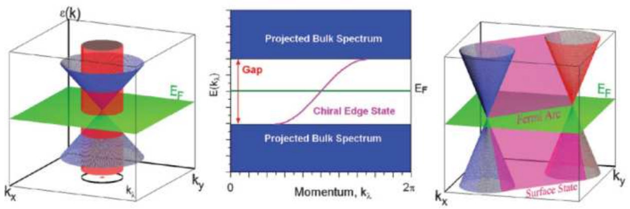

FIG. 5. (Color online) Illustration of surface states arising from bulk Weyl points. (a) The bulk states as a function of (k_x, k_y) (and arbitrary k_z) fill the inside of a cone. A cylinder whose base defines a one-dimensional circular Brillouin zone is also drawn. (b) The cylinder unrolled onto a plane gives the spectrum of the two-dimensional subsystem $H(\lambda, k_z)$ with a boundary. On top of the bulk spectrum, a chiral state appears due to the nonzero Chern number. (c) Meaning of the surface states back in the three-dimensional system. The chiral state appears as a surface connecting the original Dirac cone to a second one, and the intersection between this plane and the Fermi level gives a Fermi arc connecting the Weyl points.

PRL **109,** 066401 (2012) PHYSICAL REVIEW LETTERS

Correlation Effects on 3D Topological Phases: From Bulk to B

Ara Go,[1,2] William Witczak-Krempa,[3] Gun Sang Jeon,[2] Kwon Park,[4] and Yong

PRL **110,** 136601 (2013) PHYSICAL REVIEW LETTERS week ending 29 MARCH 2013

Topological Phase Transitions Driven by Magnetic Phase Transitions in $Fe_xBi_2Te_3$ $(0 \le x \le 0.1)$ Single Crystals

Heon-Jung Kim,[1,*] Ki-Seok Kim,[2] J.-F. Wang,[3] V. A. Kulbachinskii,[4] K. Ogawa,[5] M. Sasaki,[6] A. Ohnishi,[6] M. Kitaura,[6] Y.-Y. Wu,[3] L. Li,[3] I. Yamamoto,[5] J. Azuma,[5] M. Kamada,[5] and V. Dobrosavljević[7]

Phase diagram of $Fe_xBi_2Te_3$

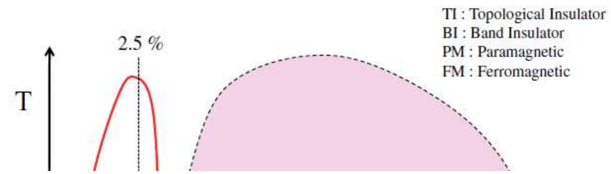

PHYSICAL REVIEW B **86**, 214514 (2012)

Superconductivity of doped Weyl semimetals: Finite-momentum pairing and electronic analog of the ^{3}He-*A* phase

Gil Young Cho,[1] Jens H. Bardarson,[1,2] Yuan-Ming Lu,[1,2] and Joel E. Moore[1,2]
[1]*Department of Physics, University of California, Berkeley, California 94720, USA*
[2]*Materials Sciences Division, Lawrence Berkeley National Laboratory, Berkeley, California 94720, USA*
(Received 15 September 2012; published 26 December 2012)

We study superconducting states of doped inversion-symmetric Weyl semimetals. Specifically, we consider a lattice model realizing a Weyl semimetal with an inversion symmetry and study the superconducting instability in the presence of a short-ranged attractive interaction. With a phonon-mediated attractive interaction, we find two competing states: a fully gapped finite-momentum Fulde-Ferrell-Larkin-Ovchinnikov pairing state and a nodal even-parity pairing state. We show that, in a BCS-type approximation, the finite-momentum pairing state is energetically favored over the usual even-parity paired state and is robust against weak disorder. Although energetically unfavorable, the even-parity pairing state provides an electronic analog of the ^{3}He-*A* phase in that the nodes of the even-parity state carry nontrivial winding numbers and therefore support a surface flat band. We briefly discuss other possible superconducting states that may be realized in Weyl semimetals.

$$\vec{E} \cdot \vec{B}$$

Anomalous transport phenomena in topological states of matter

↑

Topological terms associated with (quantum) anomalies

(Quantum) anomalies

- From classical theory to quantum theory → Nontrivial global structures of ground-state manifold sometimes violate classically respected conservation laws at quantum levels, referred to as (quantum) anomalies.
- Heisenberg vs. Feynman
- Anomalies associated with local (gauge) symmetries must be cancelled for consistency of quantum theory (standard model & string theory).
- Anomalies associated with global symmetries give rise to exotic physics.
- Quantum number fractionalization in solitons (Goldstone-Wilczek currents), deconfined quantum criticality (emergent non-abelian chiral anomaly), gapless boundary states and anomalous (quantized) electrical & thermal (Hall) transport phenomena, …
- Chiral anomaly (3+1, 1+1), parity anomaly (2+1), Witten anomaly (3+1), …

Topological (anomaly) terms vs. anomalous transport phenomena

- **Parity anomaly (Semenoff, Haldane, Fradkin, ⋯) ➔ Chern-Simons term: Quantum Hall effect**

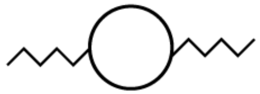

$$S = \int \bar{\psi}\left[\sigma_\mu\left(\partial_\mu + iA_\mu\right) + m\right]\psi \longrightarrow S_{\text{eff}} = \left[\frac{i\text{sgn}\,(m)}{8\pi} - \frac{i\text{sgn}\,(M)}{8\pi}\right]\int \epsilon_{\mu\nu\lambda}A_\mu\partial_\nu A_\lambda$$

- **Chiral (Adler-Bell-Jackiw) anomaly ➔ θ (E.B) term: Half-quantized Hall conductance when $\theta = \pi$ (time reversal symmetry) in topological insulators**

$$\nabla\cdot\mathbf{D} = 4\pi\rho + 2\alpha(\nabla P_3\cdot\mathbf{B}),$$

$$\nabla\times\mathbf{H} - \frac{1}{c}\frac{\partial\mathbf{D}}{\partial t} = \frac{4\pi}{c}\mathbf{j} - 2\alpha\left((\nabla P_3\times\mathbf{E}) + \frac{1}{c}(\partial_t P_3)\mathbf{B}\right),$$

$$\nabla\times\mathbf{E} + \frac{1}{c}\frac{\partial\mathbf{B}}{\partial t} = 0, \qquad \nabla\cdot\mathbf{B} = 0, \qquad (68)$$

$$S = \frac{\theta e^2}{16\pi^2 h}\int d^3x dt\,\epsilon^{\mu\nu\kappa\lambda}F_{\mu\nu}F_{\kappa\lambda} = \frac{\theta e^2}{2\pi^2 h}\int d^3x dt\,\boldsymbol{E}\cdot\boldsymbol{B}$$

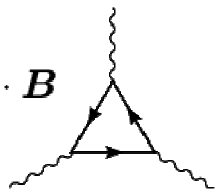

- **Delocalized gapless surface states against Anderson localization due to the presence of topological terms such as WZW, theta, and Z2 terms in the nonlinear sigma model formulation**

Adler-Bell-Jackiw anomaly (1d)

Volume 130B, number 6 PHYSICS LETTERS 3 November 1983

THE ADLER–BELL–JACKIW ANOMALY AND WEYL FERMIONS IN A CRYSTAL

H.B. NIELSEN
Niels Bohr Institute and Nordita, 17 Blegdamsvej, DK2100, Copenhagen Ø, Denmark

and

Masao NINOMIYA [1]
Department of Physics, Brown University, Providence, RI 02912, USA

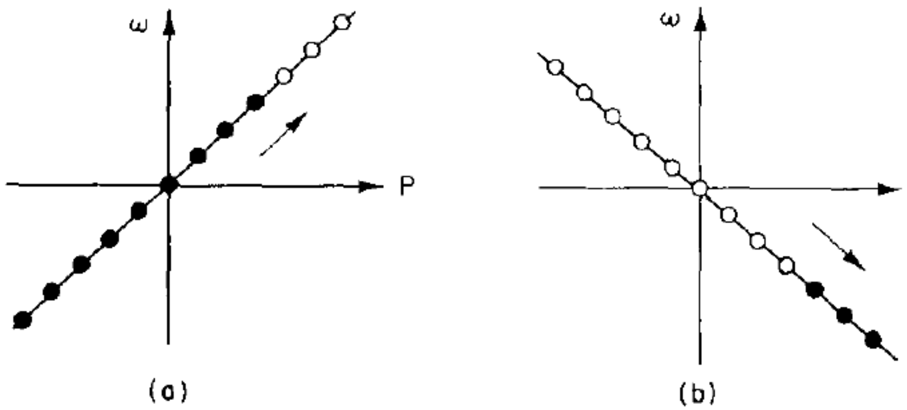

$$\dot{N}_R = \frac{e}{2\pi}E \ \& \ \dot{N}_L = -\frac{e}{2\pi}E$$

$$\dot{N}_R + \dot{N}_L = 0 \ \& \ \dot{N}_R - \dot{N}_L = \dot{Q}_5 = \frac{e}{\pi}E$$

Fig. 1. Dispersion laws for the RH (a) and LH (b) Weyl fermions in 1 + 1 dimensions. The black and white points denote the filled and unfilled levels and the arrows indicate the direction of the movement of the Fermi surface when E in on.

Weyl vs. Dirac (semimetal)

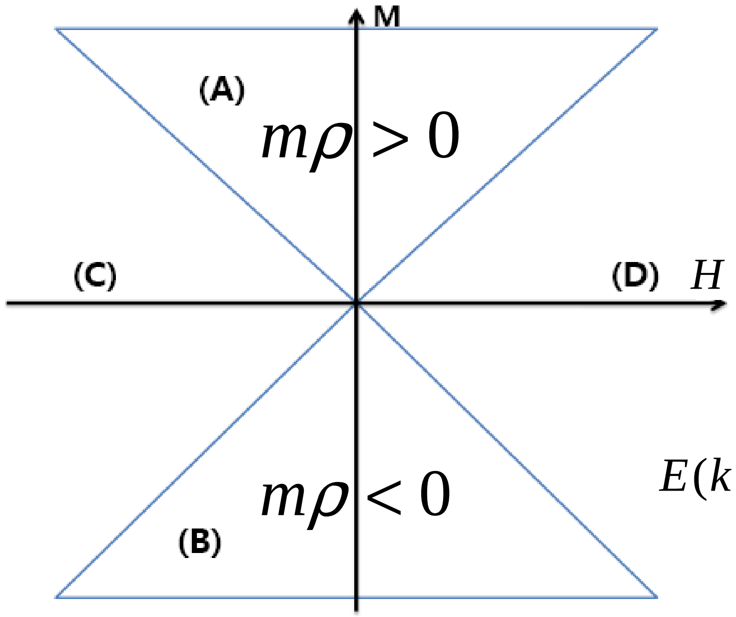

$$H = V_D k \cdot \sigma \otimes \tau^z + M(k) I \otimes \tau^x$$
$$+ gH\hat{z} \cdot \sigma \otimes I$$

$$M(k) = m - \rho k^2$$

$$E(k) = \pm\sqrt{V_D^2\left(k_x^2 + k_y^2\right) + \left(gH \pm \sqrt{M^2(k) + V_D^2 k_z^2}\right)^2}$$

FIG. 1. Proposed phase diagram in terms of $(H\ M)$ for $b < 0$ in Hamiltonian Eq.(4): (A),(B) Topological band gap M is larger than magnetization mass H, thus we are in the insulating phase. We have a topological band insulator (A) for $M > 0$ and trivial insulator (B) for $M < 0$. (C),(D) Magnetization mass is stronger than the topological band gap, and we have a Weyl semimetal phase. Note that if $H \to -H$ then two Weyl points change the sign of the chirality. At the transitions $|H| = |M|$, two Weyl points meet each other and result topological or trivial insulators.

Gil Young Cho, 1110.1939v2

Adler-Bell-Jackiw anomaly (3d): Ultra-quantum limit

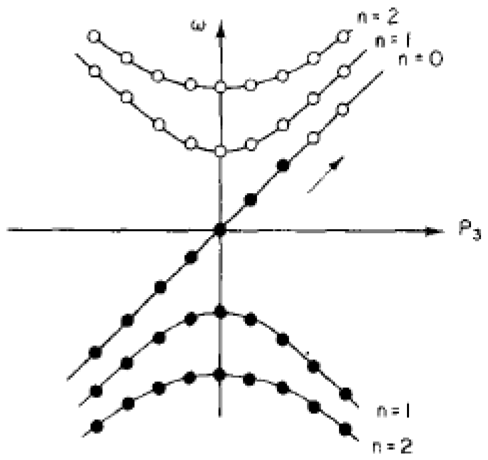

Fig. 2. Dispersion law for the RH Weyl fermion in 3 + 1 dimensions in the presence of a magnetic field in the x^3-direction.

$$\omega(n, \sigma_3, P_3) = \pm[2eH(n+\tfrac{1}{2}) + (P_3)^2 + eH\sigma_3]^{1/2}$$

$(n = 0, 1, 2, \ldots)$

except for the $n = 0$ and $\sigma_3 = -1$ mode where

$$\omega(n = 0, \sigma_3 = -1, P_3) = \pm P_3 \ .$$

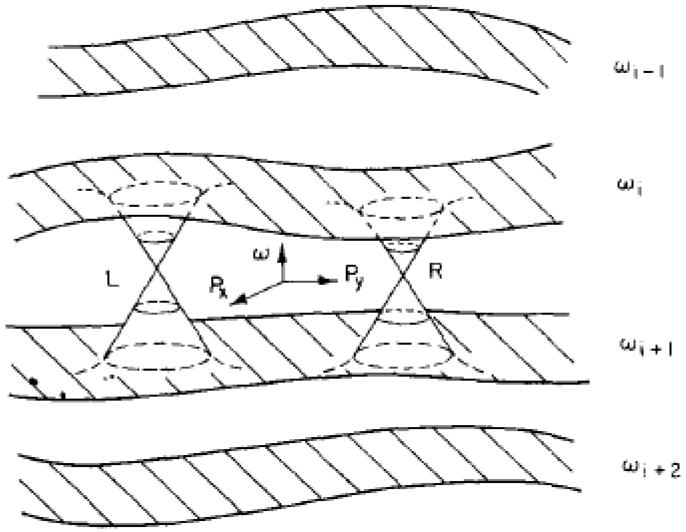

Fig. 3. Generic dispersion law for the two degeneracy points denoted by R and L between the energy levels ω_i and ω_{i+1}. The shaded surfaces in (3 + 1)-dimensional $\omega - \boldsymbol{P}$ space denote the layers of the energy bands. One momentum axis, P_z, is suppressed. Near the degeneracy points R and L, the dispersion laws are cones. The equation near R is the RH Weyl equation and the one near L is LH one.

$$\dot{N}_R = \frac{e^2}{4\pi^2}EB \ \& \ \dot{N}_L = -\frac{e^2}{4\pi^2}EB$$

$$\dot{N}_R + \dot{N}_L = 0 \ \& \ \dot{N}_R - \dot{N}_L = \dot{Q}_5 = \frac{e^2}{2\pi^2}EB$$

Adler-Bell-Jackiw anomaly (3d): Semi-classical regime

Chiral Anomaly and Classical Negative Magnetoresistance of Weyl Metals

D. T. Son[1] and B. Z. Spivak[2]

[1] *Institute for Nuclear Theory, University of Washington, Seattle, WA 98195-1550, USA*
[2] *Department of Physics, University of Washington, Seattle, WA 98195, USA*

(Dated: June 2012)

arXiv:1206.1627v1

$$\frac{\partial N^{(i)}}{\partial t} + \boldsymbol{\nabla}\cdot\mathbf{j}^{(i)} = k^{(i)}\frac{e^2}{4\pi^2\hbar^2 c}(\mathbf{E}\cdot\mathbf{B}) - \frac{\delta N^{(i)}}{\tau},$$

$$\mathbf{j}^{(i)} = \int\frac{\mathrm{d}\mathbf{p}}{(2\pi\hbar)^3}\left[\mathbf{v} + e\mathbf{E}\times\boldsymbol{\Omega}^{(i)}_{\mathbf{p}} + \frac{e}{c}(\boldsymbol{\Omega}^{(i)}_{\mathbf{p}}\cdot\mathbf{v})\mathbf{B}\right] n^{(i)}_{\mathbf{p}}$$

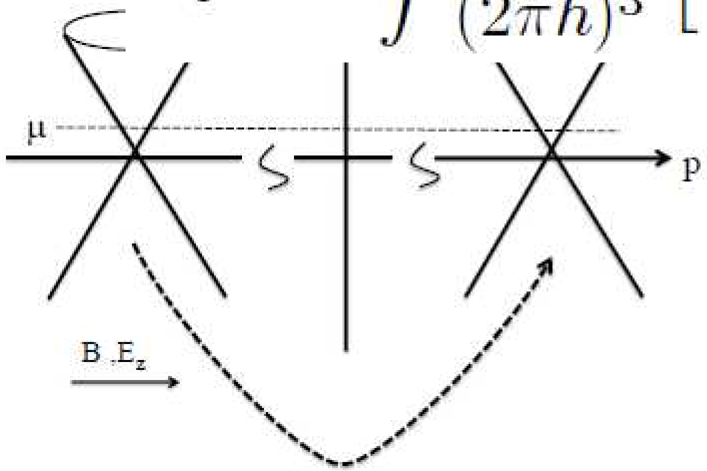

$$k^{(i)} = \frac{1}{2\pi\hbar}\oint \mathrm{d}\mathbf{S}\cdot\boldsymbol{\Omega}^{(i)}_{\mathbf{p}} = 0, \pm 1, \ldots.$$

Magnetoelectric effect

- Local curvature effect vs. global topological effect
- Local curvature effect ➔ Transverse (inverse AC effect) phenomena vs. longitudinal (magneto-elastic coupling) phenomena
- Global "topological" effect ➔ Longitudinal phenomena from the chiral anomaly (axion electrodynamics – Wilczek)

$$\nabla \cdot \mathbf{D} = 4\pi\rho + 2\alpha(\nabla P_3 \cdot \mathbf{B}),$$

$$\nabla \times \mathbf{H} - \frac{1}{c}\frac{\partial \mathbf{D}}{\partial t} = \frac{4\pi}{c}\mathbf{j} - 2\alpha\left((\nabla P_3 \times \mathbf{E}) + \frac{1}{c}(\partial_t P_3)\mathbf{B}\right),$$

$$\nabla \times \mathbf{E} + \frac{1}{c}\frac{\partial \mathbf{B}}{\partial t} = 0, \qquad \nabla \cdot \mathbf{B} = 0, \qquad (68)$$

“Negative” longitudinal magnetoresistivity

$$\vec{E} \cdot \vec{B}$$

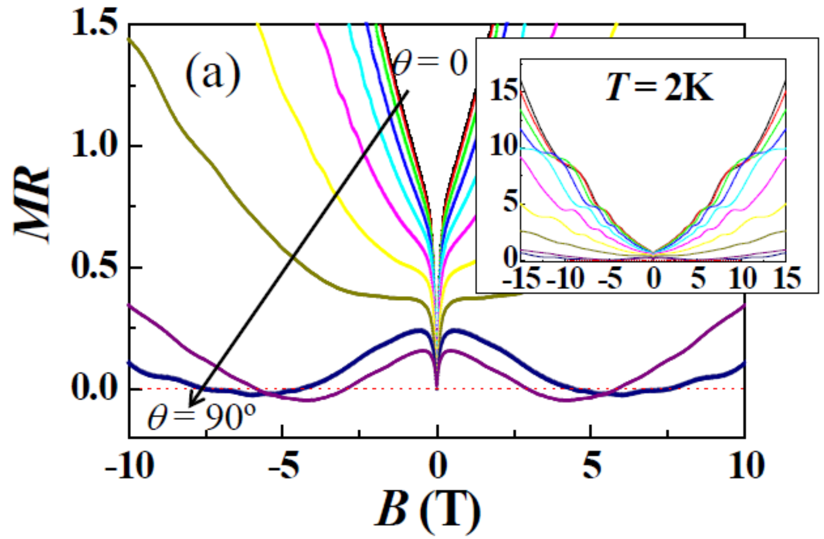

Adler-Bell-Jackiw anomaly in Weyl metals

Longitudinal magnetoresistivity

$$E_\alpha = \rho_{\alpha\beta}(B_\gamma) J_\beta$$

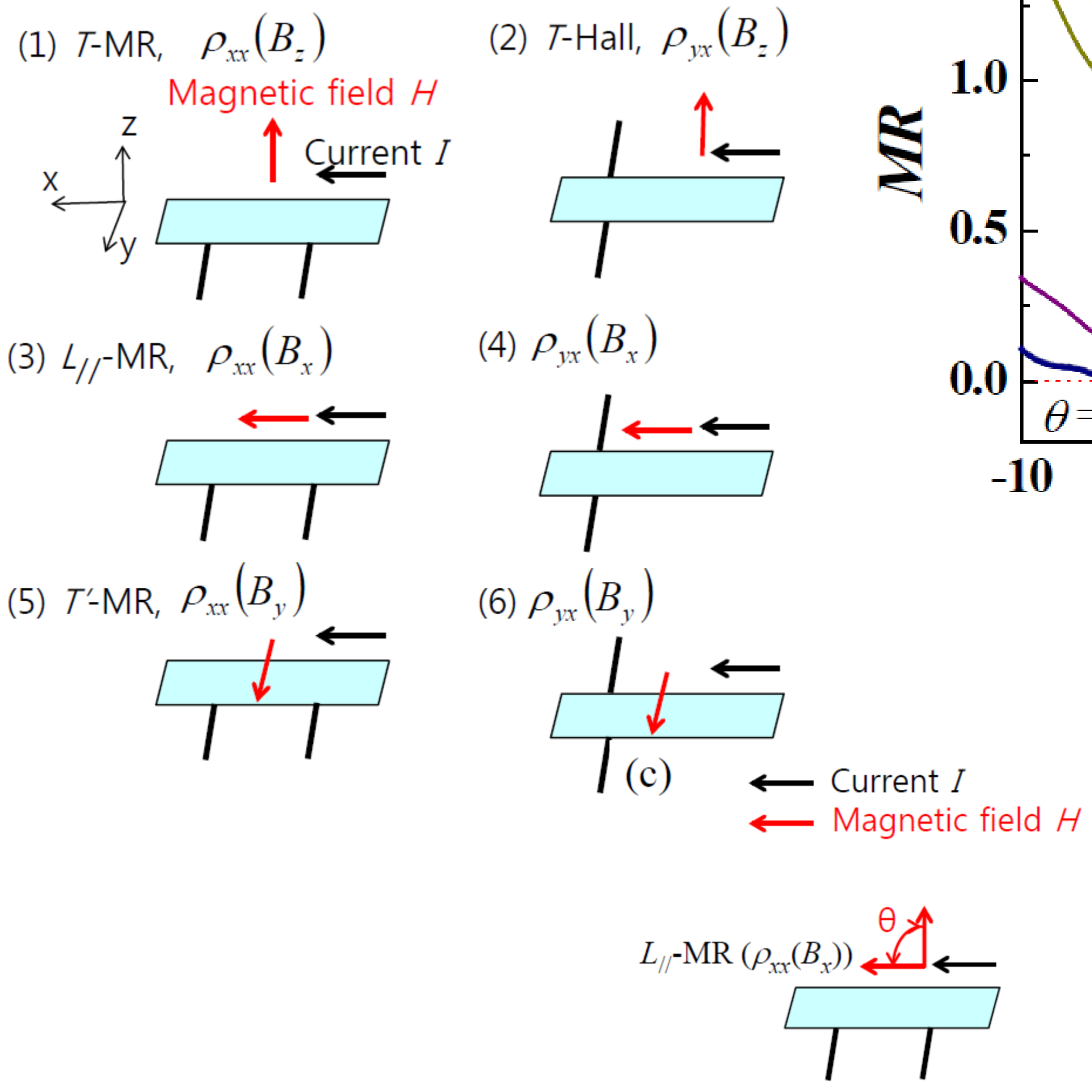

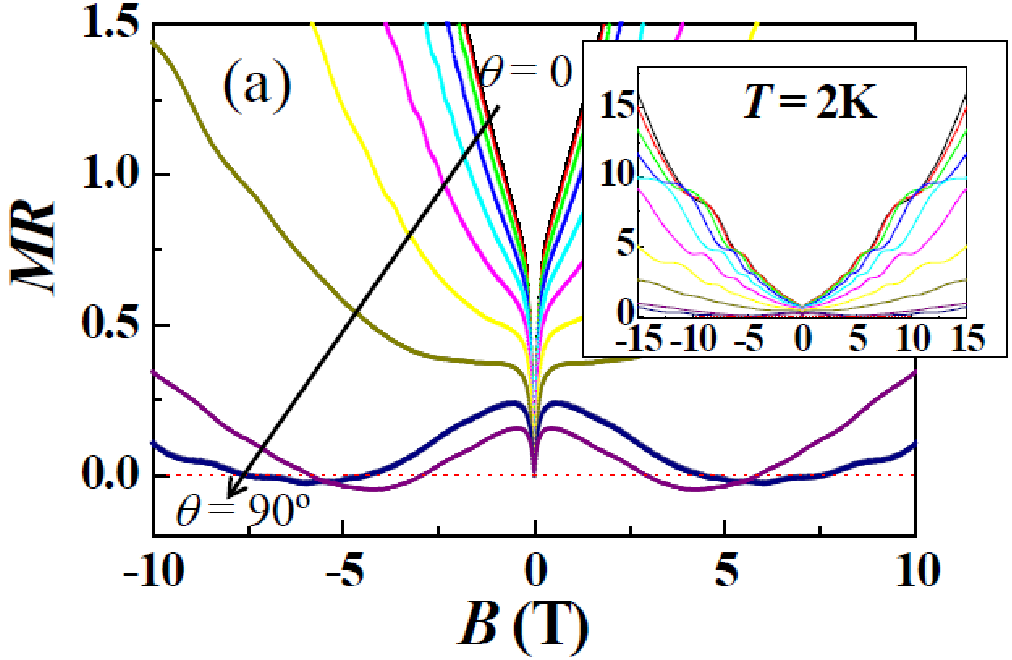

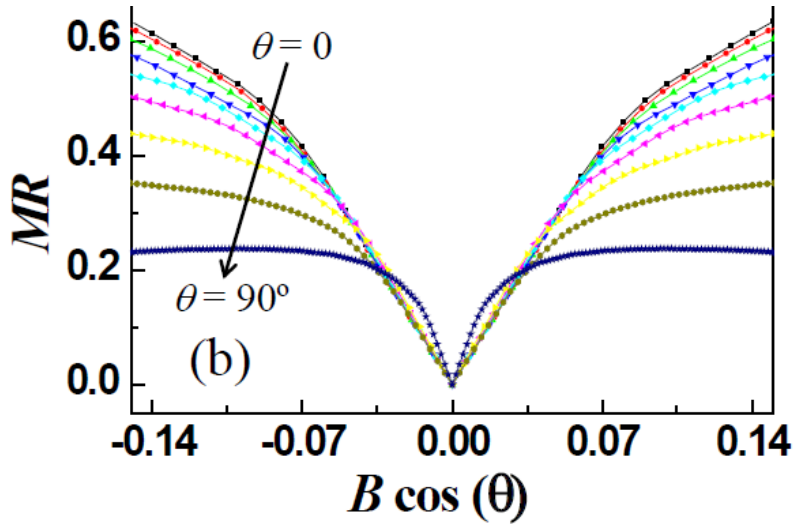

Theoretical analysis

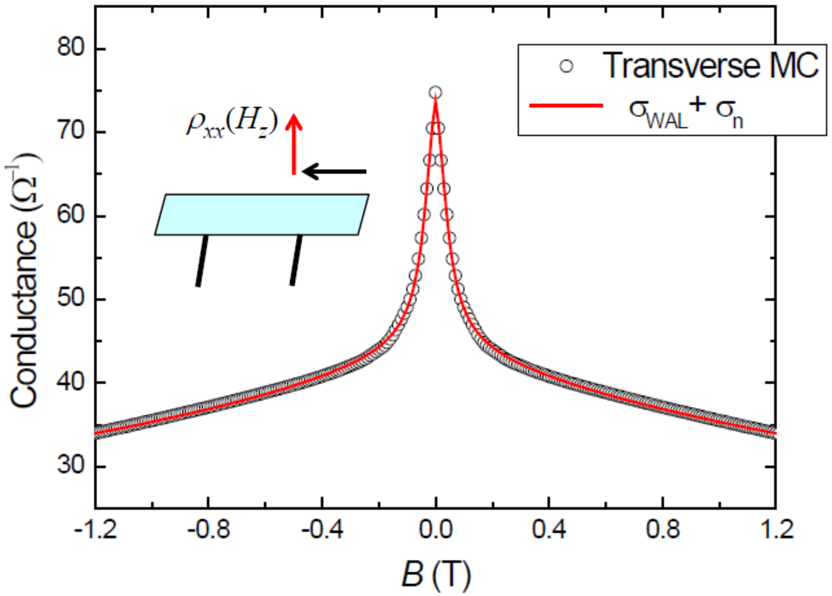

$$\sigma(B) = (\sigma_{WAL} + \sigma_n)$$

$$\sigma_{WAL} = a\sqrt{B} + \sigma_0$$

$$\sigma_n = \frac{1}{A \cdot B^2 + \rho_0}$$

a=-14.3 Ω^{-1}·$T^{-0.5}$

A=21.8 Ω·T^{-2}

ρ_0=0.0415 Ω

σ_0=49.6 Ω^{-1}

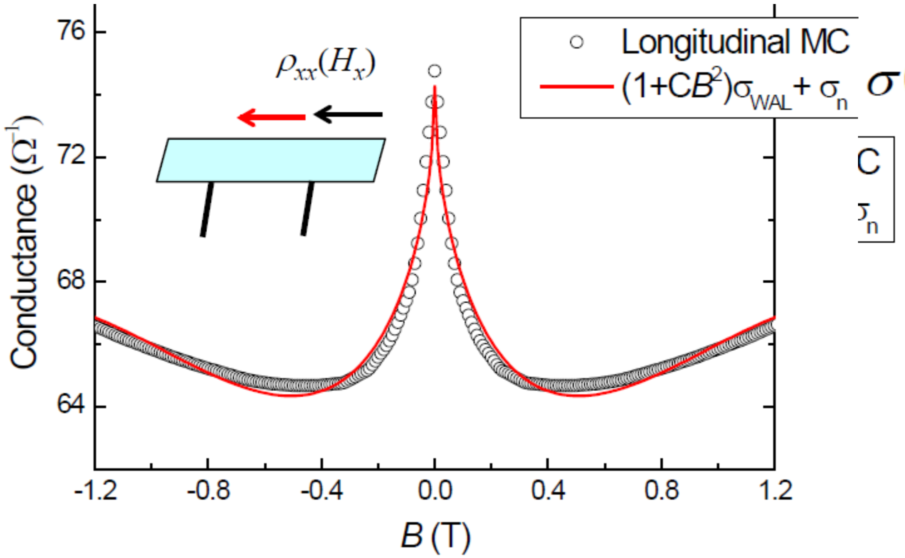

$$\sigma(B) = (1 + C_W \cdot B^2) \cdot \sigma_{WAL} + \sigma_n$$

$$\sigma_{WAL} = a\sqrt{B} + \sigma_0$$

$$\sigma_n = \frac{1}{A \cdot B^2 + \rho_0}$$

a=-20.6 Ω^{-1}·$T^{-0.5}$

A=0.0073 Ω·T^{-2}

C_W=1.27 T^{-2}

ρ_0=0.0265 Ω

σ_0=36.6 Ω^{-1}

Theory: Lorentz force + Berry curvature in 3d (in the absence of weak anti-localization)

$$\dot{\boldsymbol{r}} = \frac{\partial \epsilon_{\boldsymbol{p}}}{\partial \boldsymbol{p}} + \dot{\boldsymbol{p}} \times \boldsymbol{\Omega}_{\boldsymbol{p}}, \qquad \dot{\boldsymbol{p}} = \left(1 + \frac{e}{c}\boldsymbol{B}\cdot\boldsymbol{\Omega}_{\boldsymbol{p}}\right)^{-1}\left\{e\boldsymbol{E} + \frac{e}{mc}\boldsymbol{p}\times\boldsymbol{B} + \frac{e^2}{c}(\boldsymbol{E}\cdot\boldsymbol{B})\boldsymbol{\Omega}_{\boldsymbol{p}}\right\} = -\frac{\boldsymbol{p}}{\tau},$$

$$\dot{\boldsymbol{p}} = e\boldsymbol{E} + \frac{e}{c}\dot{\boldsymbol{r}} \times \boldsymbol{B}, \qquad \boldsymbol{J} = ne\dot{\boldsymbol{r}} = ne\left(1 + \frac{e}{c}\boldsymbol{B}\cdot\boldsymbol{\Omega}_{\boldsymbol{p}}\right)^{-1}\left\{\frac{\boldsymbol{p}}{m} + e\boldsymbol{E}\times\boldsymbol{\Omega}_{\boldsymbol{p}} + \frac{e}{mc}(\boldsymbol{\Omega}_{\boldsymbol{p}}\cdot\mathbf{p})\boldsymbol{B}\right\}$$

$$-\frac{p_x}{\tau} = \left(1 + \frac{e}{c}B_x\Omega^x_{\boldsymbol{p}}\right)^{-1}\left\{eE_x + \frac{e^2}{c}(E_xB_x)\Omega^x_{\boldsymbol{p}}\right\},$$

$$-\frac{p_y}{\tau} = \left(1 + \frac{e}{c}B_x\Omega^x_{\boldsymbol{p}}\right)^{-1}\left\{eE_y + \omega^x_c p_z + \frac{e^2}{c}(E_xB_x)\Omega^y_{\boldsymbol{p}}\right\},$$

$$-\frac{p_z}{\tau} = \left(1 + \frac{e}{c}B_x\Omega^x_{\boldsymbol{p}}\right)^{-1}\left\{-\omega^x_c p_y + \frac{e^2}{c}(E_xB_x)\Omega^z_{\boldsymbol{p}}\right\},$$

$$\boldsymbol{\Omega}_{\mathbf{p}} = \boldsymbol{\nabla}_{\mathbf{p}} \times \mathbf{A}_{\mathbf{p}}, \qquad \mathbf{A}_{\mathbf{p}} = i\langle u_{\mathbf{p}}|\boldsymbol{\nabla}_{\mathbf{p}} u_{\mathbf{p}}\rangle,$$

Xiao, D., Chang, M.-C. & Niu, Q.
Berry phase effects on electronic properties, Rev. Mod. Phys. 82, 1959 (2010);
Nagaosa, N., Sinova, J., Onoda, S., MacDonald, A. H. & Ong, N. P. Anomalous Hall effect,
Rev. Mod. Phys. 82, 1539 (2010).

$$J_y = ne\left(1 + \frac{e}{c}B_x\Omega^x_{\boldsymbol{p}}\right)^{-1}\left(\frac{p_y}{m} - eE_x\Omega^z_{\boldsymbol{p}}\right) \longrightarrow 0$$

$$p_x = -e\tau E_x,$$

$$p_y = em\Omega^z_{\boldsymbol{p}}E_x$$

$$p_z = e\tau\left(1 + \frac{e}{c}B_x\Omega^x_{\boldsymbol{p}}\right)^{-1}\left(\frac{e}{c}\Omega^z_{\boldsymbol{p}}E_x - \frac{e}{c}(E_xB_x)\Omega^z_{\boldsymbol{p}}\right)$$

$$E_y = -\frac{m}{\tau}\Omega^z_{\boldsymbol{p}}\left(1 + \frac{e}{c}B_x\Omega^x_{\boldsymbol{p}}\right)\left\{1 + \left(1 + \frac{e}{c}B_x\Omega^x_{\boldsymbol{p}}\right)^{-2}(\omega^x_c\tau)^2\right\}E_x$$
$$+\frac{e}{c}\left\{(\omega^x_c\tau)\left(1 + \frac{e}{c}B_x\Omega^x_{\boldsymbol{p}}\right)^{-1}\Omega^z_{\boldsymbol{p}} - \Omega^y_{\boldsymbol{p}}\right\}(E_xB_x).$$

$$J_x = ne\left(1 + \frac{e}{c}B_x\Omega^x_{\boldsymbol{p}}\right)^{-1}\left\{\frac{p_x}{m} + \frac{e}{mc}(\boldsymbol{\Omega}_{\boldsymbol{p}}\cdot\mathbf{p})B_x\right\}$$

Theory: Quantum Boltzmann equation approach + semi-classical equation of motion (for weak anti-localization)

$$\dot{\boldsymbol{p}} \cdot \frac{\partial G^<(\boldsymbol{p},\omega)}{\partial \boldsymbol{p}} + \dot{\boldsymbol{r}} \cdot \dot{\boldsymbol{p}} \frac{\partial G^<(\boldsymbol{p},\omega)}{\partial \omega} - \dot{\boldsymbol{p}} \cdot \left\{ \frac{\partial \Sigma^<(\boldsymbol{p},\omega)}{\partial \omega} \frac{\partial \Re G_{ret}(\boldsymbol{p},\omega)}{\partial \boldsymbol{p}} - \frac{\partial \Re G_{ret}(\boldsymbol{p},\omega)}{\partial \omega} \frac{\partial \Sigma^<(\boldsymbol{p},\omega)}{\partial \boldsymbol{p}} \right\}$$
$$= -2\Gamma(\boldsymbol{p},\omega) G^<(\boldsymbol{p},\omega) + \Sigma^<(\boldsymbol{p},\omega) A(\boldsymbol{p},\omega). \qquad (2)$$

$$\dot{\boldsymbol{r}} = \frac{\partial \epsilon_{\boldsymbol{p}}}{\partial \boldsymbol{p}} + \dot{\boldsymbol{p}} \times \boldsymbol{\Omega}_{\boldsymbol{p}}, \qquad \dot{\boldsymbol{r}} = \left(1 + \frac{e}{c} \boldsymbol{B} \cdot \boldsymbol{\Omega}_{\boldsymbol{p}}\right)^{-1} \left\{ \boldsymbol{v}_{\boldsymbol{p}} + e\boldsymbol{E} \times \boldsymbol{\Omega}_{\boldsymbol{p}} + \frac{e}{c} \boldsymbol{\Omega}_{\boldsymbol{p}} \cdot \boldsymbol{v}_{\boldsymbol{p}} \boldsymbol{B} \right\},$$

$$\dot{\boldsymbol{p}} = e\boldsymbol{E} + \frac{e}{c} \dot{\boldsymbol{r}} \times \boldsymbol{B}, \qquad \dot{\boldsymbol{p}} = \left(1 + \frac{e}{c} \boldsymbol{B} \cdot \boldsymbol{\Omega}_{\boldsymbol{p}}\right)^{-1} \left\{ e\boldsymbol{E} + \frac{e}{c} \boldsymbol{v}_{\boldsymbol{p}} \times \boldsymbol{B} + \frac{e^2}{c} (\boldsymbol{E} \cdot \boldsymbol{B}) \boldsymbol{\Omega}_{\boldsymbol{p}} \right\}.$$

$$\boldsymbol{J} = -e \frac{1}{\beta} \sum_{i\omega} \int \frac{d^3 \boldsymbol{p}}{(2\pi\hbar)^3} \left(1 + \frac{e}{c} \boldsymbol{B} \cdot \boldsymbol{\Omega}_{\boldsymbol{p}}\right)^{-1} \left\{ \boldsymbol{v}_{\boldsymbol{p}} + e\boldsymbol{E} \times \boldsymbol{\Omega}_{\boldsymbol{p}} + \frac{e}{c} (\boldsymbol{\Omega}_{\boldsymbol{p}} \cdot \boldsymbol{v}_{\boldsymbol{p}}) \boldsymbol{B} \right\} [-iG^<(\boldsymbol{p}, i\omega)]$$

Final expression of longitudinal MR

$$\sigma^{L}_{exp}(B_x) = \frac{\sigma_L(B_x) + \sigma_L(-B_x)}{2} \approx (1 + \mathcal{C}_W B_x^2)\sigma_n(T)$$

$$\sigma_n(T) \;=\; \mathcal{C} N_F e^2 v_F^2 \tau_{tr}(T)$$

$$\sigma_L(B_x, T) = (1 + \mathcal{C}_W B_x^2)\sigma_{WAL}(B_x, T) + \sigma_n(T)$$

$$\vec{E} \cdot \vec{B}$$

Discussion: Ultra-quantum limit vs. semi-classical regime

- Semi-classical regime: Chemical potential is much larger than the cyclotron frequency.

- Ultra-quantum limit: Both chemical potential and temperature are less than the energy gap between the lowest and first Landau levels.

- Since only chiral branches of the spectrum are occupied, dynamics of these electrons are essentially the same as that of one-dimensional chiral fermions, where intra-node scattering is prohibited. As a result, the effect of the Adler-Bell-Jackiw anomaly becomes enhanced, where the longitudinal current can be relaxed by inter-node scattering only. In this ultra-quantum limit, the correction term of the longitudinal MC is linearly proportional to B due to one-dimensional chiral dynamics, distinguished from the case of the semi-classical regime.

- All analysis based on the ultra-quantum limit failed to explain our experimental data consistently, indicating that

"Topological" Hall effect

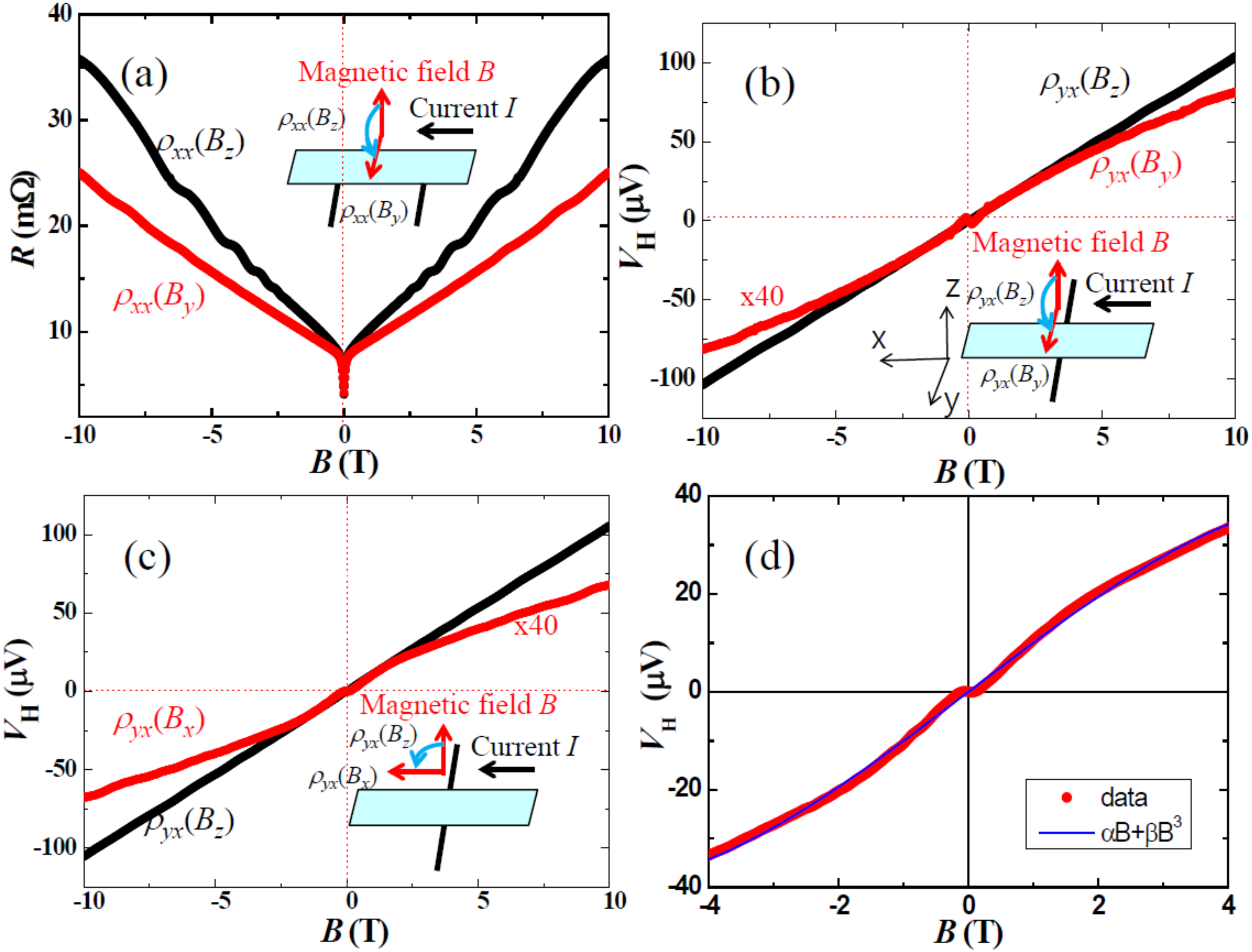

Conclusion

- Claim: Dirac metal + time reversal symmetry breaking
  ➔ Weyl metal
- Experimental observation: "Negative" longitudinal magnetoresistivity & "topological" longitudinal and transverse Hall effects
- Explanation: Dynamics of these Weyl fermions is constrained topologically when their currents are applied in the same direction as the momentum to connect the two Weyl points, referred to as the Adler-Bell-Jackiw anomaly and described by the topological $\theta\ (E \cdot B)$ term.

Confirmation of Weyl metal

Figure 1(a) Schematic band structure of $Bi_{1-x}Sb_x$ near the L point

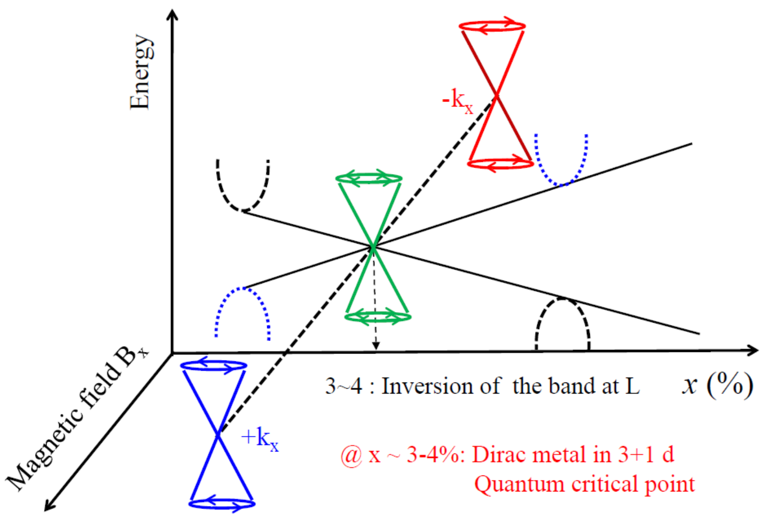

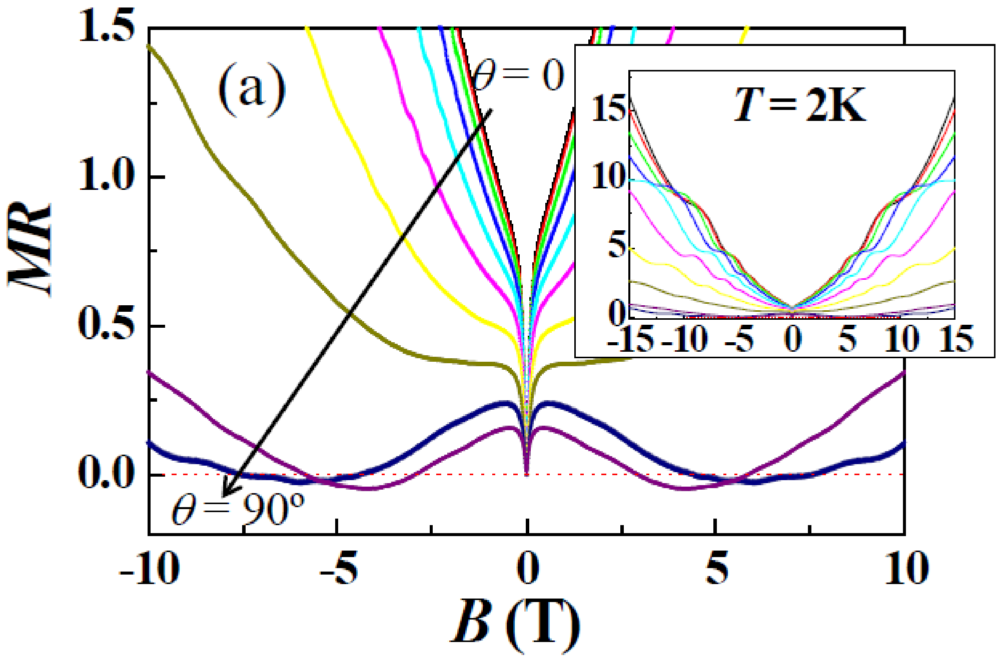

(c)

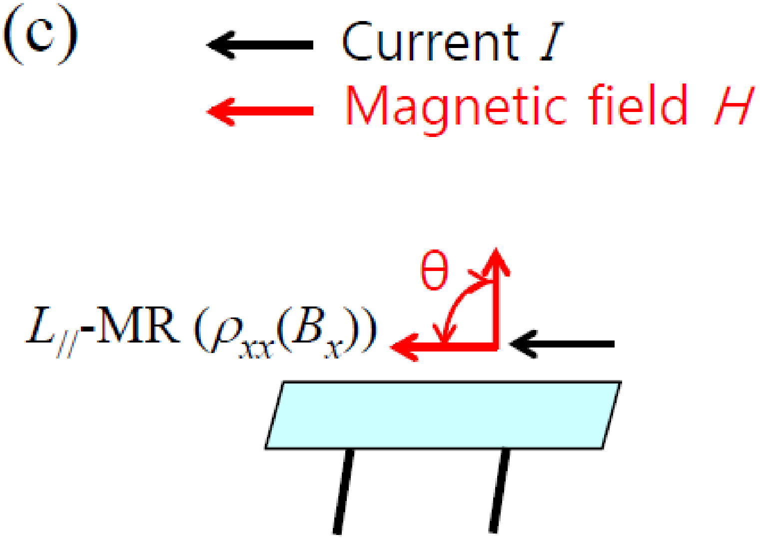

From S. Ryu's talk in APCTP

$$\pi_2(\mathrm{U}(2N)/\mathrm{U}(N)\times\mathrm{U}(N))=\mathbb{Z}$$

Field theory (Pruisken):

σ-model with topological term

$$S=\sigma_{xx}\int d^2r\,\mathrm{tr}\,[\partial_\mu Q\partial_\mu Q]+i\theta S_{\mathrm{top}}$$

$$S_{\mathrm{top}}=\frac{1}{16\pi i}\int d^2r\,\epsilon^{\mu\nu}\mathrm{tr}\,[Q\partial_\mu Q\partial_\nu Q]\in\mathbb{Z}$$

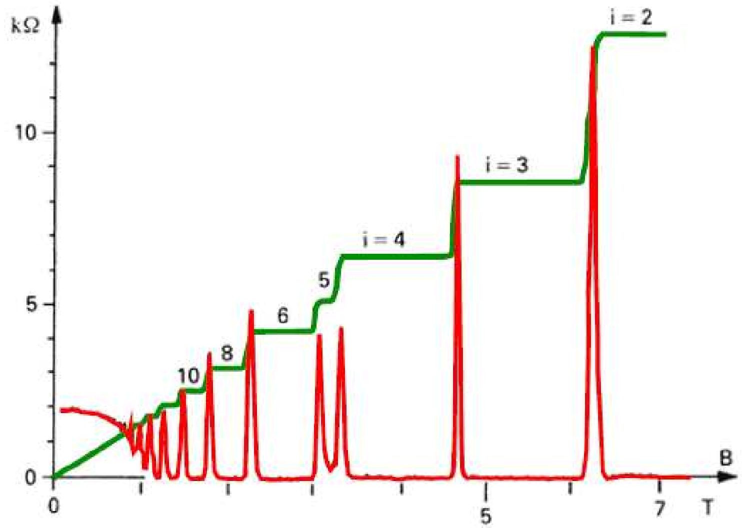

von Klitzing '80 ; Nobel Prize '85

- topological term = phase of fermionic determinant

- for the Dirac model, topological term can be computed from chiral anomaly

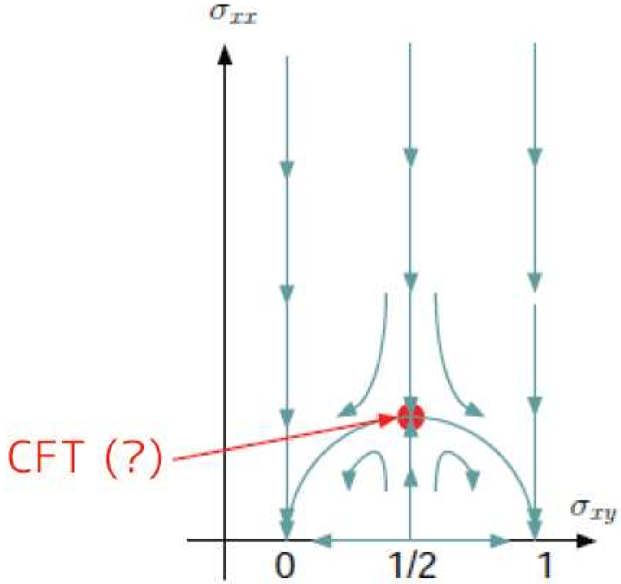

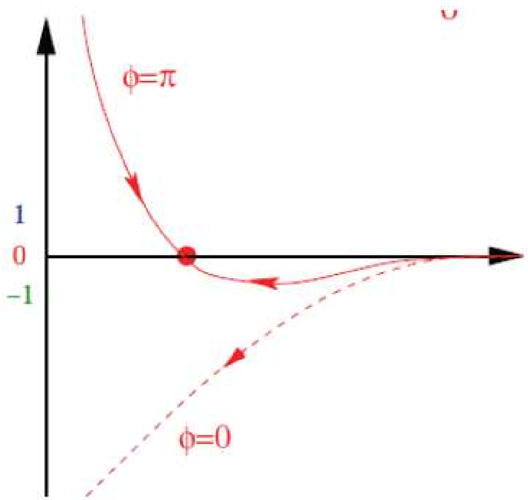

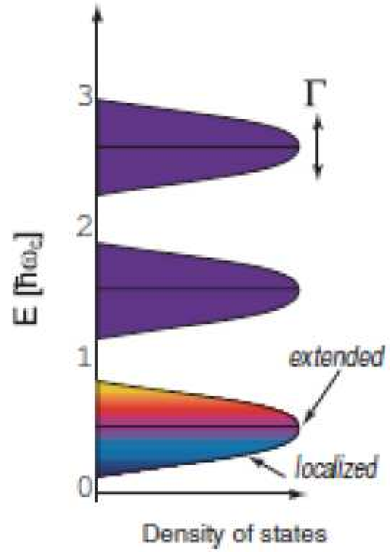

SR, Mudry, Obuse, Furusaki (07)

From S. Ryu's talk in APCTP

microscopic model:

$$\mathcal{H} = v_F\,(\sigma_x p_x + \sigma_y p_y) + V(\mathbf{r})$$

$$i\sigma_y \mathcal{H}^*(-i\sigma_y) = \mathcal{H}$$

effective field theory: non-linear sigma model

(diffusive motion of electrons)

$$Q(\mathbf{r}) \in \mathrm{O}(4N)/[\mathrm{O}(2N)\times\mathrm{O}(2N)]$$

$$S = \sigma_{xx}\int d^2r\,\mathrm{tr}\,[\partial_\mu Q \partial_\mu Q] \qquad \pi_2(\mathrm{O}(4N)/\mathrm{O}(2N)\times\mathrm{O}(2N)) = \mathbb{Z}_2$$

even number of Dirac

$$Z = \int \mathcal{D}[Q] e^{-S}$$

odd number of Dirac
-> Z2 topological term

$$Z = \int \mathcal{D}[Q](-1)^{n[Q]} e^{-S} \quad n[Q] = 0, 1$$

odd number

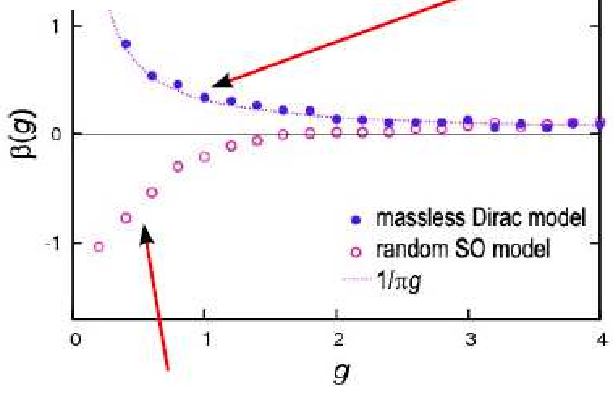

surface of 3D Z2 top. insulator = perfect metal !
"topological metal"